



UNIVERSITY OF LEEDS

This is a repository copy of *Erosion and Mobilisation of Highly Active Simulant Suspensions using Impinging Vertical Jets*.

White Rose Research Online URL for this paper:
<http://eprints.whiterose.ac.uk/150300/>

Version: Accepted Version

Proceedings Paper:

Croft, J, Peakall, J orcid.org/0000-0003-3382-4578, Rice, H et al. (1 more author) (2019) Erosion and Mobilisation of Highly Active Simulant Suspensions using Impinging Vertical Jets. In: WM2019 Conference Proceedings. WM2019: 45th annual Waste Management Symposia, 03-07 Mar 2019, Phoenix, Arizona, USA. . ISBN 978-0-9828171-9-3

This is an author produced version of a conference paper published in WM2019 Conference Proceedings. Uploaded with permission from the publisher.

Reuse

Items deposited in White Rose Research Online are protected by copyright, with all rights reserved unless indicated otherwise. They may be downloaded and/or printed for private study, or other acts as permitted by national copyright laws. The publisher or other rights holders may allow further reproduction and re-use of the full text version. This is indicated by the licence information on the White Rose Research Online record for the item.

Takedown

If you consider content in White Rose Research Online to be in breach of UK law, please notify us by emailing eprints@whiterose.ac.uk including the URL of the record and the reason for the withdrawal request.



eprints@whiterose.ac.uk
<https://eprints.whiterose.ac.uk/>

**Erosion and Mobilisation of Highly Active Simulant Suspensions using Impinging Vertical Jets –
19378**

Joshua Croft*, Jeff Peakall**, Hugh Rice* and Timothy Hunter*

* School of Chemical and Process Engineering, University of Leeds, UK

** School of Earth and Environment, University of Leeds, UK

ABSTRACT

Based on the nuclear industry in the U.K., storage of nuclear waste poses a particularly complex challenge. Specifically, this research is concerned with post-PUREX (Plutonium Uranium Redox EXtraction) high level waste, known as HAL (Highly Active Liquor), containing nitric acid and a host of fission products. HAL is concentrated, and stored in HASTs (Highly Active Storage Tanks) at the HALES (Highly Active Liquor Evaporation and Storage) facility at the Sellafield site, UK. HASTs are large concrete containers designed to keep the HAL cool and continually circulated prior to vitrification for permanent storage and disposal. Without comprehensive understanding of how this HAL is behaving within the HASTs, a multitude of issues could arise, and understanding such issues is the basis of this research. Components of the HAL begin to form solid particles in the HASTs, and impinging vertical liquid jets are used to mobilize the sedimented particle bed to reduce hot-spot formation. Experimental validation of the jets and associated modelling is required to assess the jets efficacy, and by considering the erosion based on dimensionless parameters, will allow the results to be scaled. This is of particular interest due to the wide reaching applications to all industries that require utilisation of impinging jets, for mass or heat transfer.

An experimental rig of 0.5 m³ has been used to experimentally model the central jet of the HASTs. A spherical glass simulant (SiO₂, spherical) of various sizes has been used for the initial non-cohesive particle testing, and modelling. Each experiment used 8 different jet diameters. Dimensionless analysis takes the form of the erosion parameter, E_c , which allows comparison of systems of different scales and a means of correlating multiple simulants against one another, so patterns are easily identifiable. Part of the dimensionless analysis was also to deduce the modified Shields parameter from vane viscometry to allow for a comparison of erosion behaviour taking into account particle properties, flow properties and the overall influence these have on the erosion profile. Particle size distribution was found to have a direct effect on yield stress and modified Shields parameter, with larger particles being dominated by inertial forces and past a certain size threshold surface forces appear to dominate. E_c data found the larger glass simulants to behave as expected for a non-cohesive particles, however surface forces also appear to be present for the smaller size distributions.

INTRODUCTION

The UK's first venture into nuclear power was the Calder Hall facility in 1952 [1]. Since this date, nuclear waste has been generated. Along with electricity production, part of the purpose of this nuclear programme was to generate plutonium. The means to access the plutonium in the spent nuclear fuel was through reprocessing. The spent nuclear fuel is dissolved in nitric acid, allowing the uranium and plutonium to be selectively removed from the waste stream using solvent extraction (i.e. PUREX). This process leaves behind the majority of the remaining fission products in solution (highly active liquor). This solution is evaporated to form a concentrate at HALES at Sellafield, and subsequently stored in one of 21 HASTs. Using only "Newside" HASTs (displayed in Fig. 1, adapted from [2]) for any new liquor [3]. This is an interim storage method prior to the liquor being vitrified into an immobile stable glass waste-form and permanently stored in a geological disposal facility (still under planning), constituting part of ongoing post operational clean out [4].

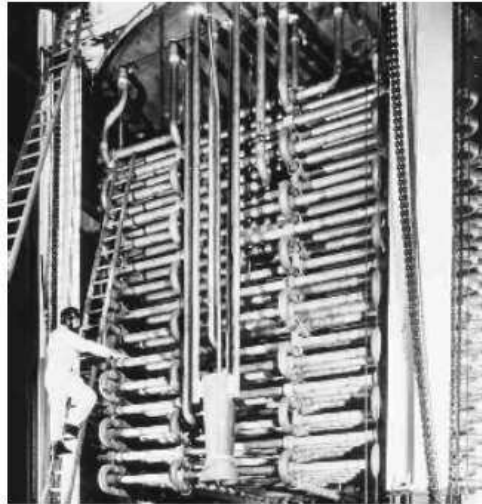


Fig. 1. Newside HAST internals [2]

During the liquor's interim storage within the HASTs it must be kept cool and circulating as it is high level waste. Meaning it is both radioactive and heat generating (20-460 kW and 37 GBq mL⁻¹ from at least 10% Cs-137 [5, 6]). To ensure no damage is caused to the HASTs, each Newside vessel contains air-lifts and impinging jets to ensure thorough mixing around the cooling coils (horizontal pipes visible in Fig. 1). They also facilitate resuspension of any precipitates that are formed. Known precipitates include caesium phosphomolybdate ($\text{Cs}_3\text{PMo}_{12}\text{O}_{40}\cdot x\text{H}_2\text{O}$) (CPM) and zirconium molybdate ($[\text{ZrMo}_2\text{O}_7(\text{OH})_2]\cdot 2\text{H}_2\text{O}$) (ZM) [7], and if allowed to settle to the base of the HASTs could form a sediment bed that becomes impossible to resuspend, resulting in hot-spots that cause damage to the HASTs.

The liquor properties are becoming increasingly well understood, as the requirements of post operational clean-out demand it [8]. The effect the impinging jets have upon any settled material is not well known due to the risk concerned with direct measurements of the HAST internals, leading to the requirement of experimentally investigating the impinging jets' effect on non-radioactive simulants. Each HAST has seven impinging jets, six wall jets and one central jet as displayed in Fig. 2 (adapted from [2]). Each wall impinging jet will have more complicated interactions with any settled bed of particles due to wall effects [9]. Experimental examination of the central jet is the most pressing issue, as it can be used to infer the efficacy of the wall jets considering it will have the greatest area of effect on any settled particles.

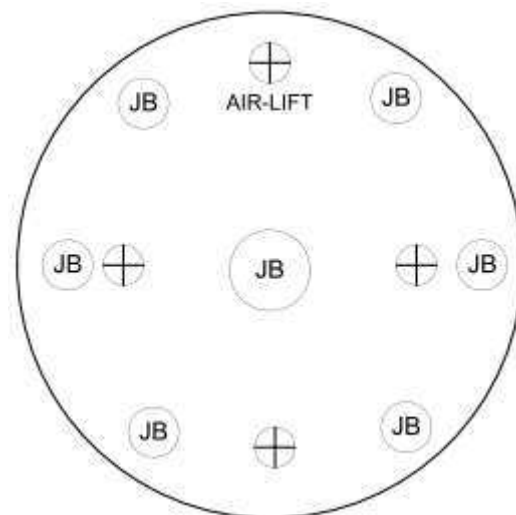


Fig. 2 Schematic of air-lifts and jets [2]

ZM and CPM are prone to form colloidal particles and aggregate [10]. Under normal circumstances cohesive particles are much harder to resuspend via erosion than non-cohesive particles [11]. This is due to cohesive particles propensity to aggregate, and thus are liable to form networked bonds if allowed to form settled beds. At what point smaller size distributions of non-cohesive particles start to display cohesive behaviour and differing erosion profiles is particularly hard to distinguish from their expected behaviour of the larger size distributions. Understanding how non-cohesive particles behave under the influence of an impinging jet is therefore paramount to act as a standard by which to determine exactly how cohesive particles differ under the experimental conditions. It has been observed that there are differences between cohesive and non-cohesive particles, yet no clear reasoning as to what might be the cause [12].

To test this, an experimental rig of 0.5 m³ has been used to experimentally model the central jet of the HASTs. A spherical glass simulant (SiO₂, spherical) of various sizes has been used for the initial non-cohesive particle testing, and modelling. Each experiment used 8 different jet diameters. Analysis took the form of the erosion parameter, E_c , which allows comparison of systems of different scales and a means of correlating multiple simulants against one another, so patterns are easily identifiable. Part of the dimensionless analysis was also to deduce the modified Shields parameter from vane viscometry to allow for a comparison of erosion behaviour taking into account particle properties and the overall influence these have on the erosion profile. Particle size distribution was found to have a direct effect on yield stress and modified Shields parameter, with larger particles being dominated by inertial forces and past a certain size threshold surface forces appear to dominate. E_c data found the larger glass simulants to behave as expected for a non-cohesive particles, however surface forces also appear to be present for the smaller size distributions.

THEORY

Dimensionless Analysis

Understanding how impinging jets behave is crucial to determining their efficacy within the HASTs. An impinging jet has three distinct regions: the free jet region, where the jet core potential exists (up to 95% of the jet tip escape velocity, up to 6 diameters, 6d, of the jet nozzle); the impingement region or fully developed flow region; and the wall jet region after deflection off a surface [13-15]. The impinging jets within the HASTs are approximately at 10d from the surface of any settled material [2], which can be considered a compromise between the jet core potential distance and the area of effect. The conditions under which an impinging jet operates can only be compared to the same set of conditions. A method of dimensionless analysis is required to compare systems of scale. Such a method was derived by Aderibigbe and Rajaratnam [14], and the erosion parameter (E_c , Eq. 1) is defined as follows:

$$E_c = \frac{U_0(d/h)}{\sqrt{gD(\Delta\rho/\rho_f)}}, \quad (\text{Eq. 1})$$

where U_0 = Jet tip velocity, d = jet tip diameter, h = height of jet tip above surface of bed, g = acceleration due to gravity, D = diameter of particles, $\Delta\rho$ = difference in fluid and particle density, and ρ_f = fluid density. E_c represents inertial forces over the tendency of the settled bed to resistance external forces (i.e. the jet). Using E_c allows for the HAST jets to be analysed realistically on a much smaller scale [16].

Aderibigbe and Rajaratnam [14] report two distinct erosion regimes exist for impinging jets, the strongly deflected jet regime (SDJR) and weakly deflected jet regime (WDJR). $E_c < 2$ represents the weakly deflected jet regime, and $E_c > 2$ the strongly deflected jet regime. For non-cohesive particles at $E_c > 2$, a

linear relationship is to be expected. Simply, the more energy the jet has (velocity), the more force is applied to the bed and particles in the form of shear stress, causing more erosion.

Considered with E_c is the dimensionless shear stress, the Shields parameter (Eq. 2) [17, 18]:

$$\tau_* = \frac{\tau}{(\rho_s - \rho_f)gD}, \quad (\text{Eq. 2})$$

where τ_* = dimensionless shear stress, this is the Shields number/parameter and τ = shear stress, D = diameter of particles, ρ_s = particle density, and ρ_f = fluid density. Particle diameter and density alone are not sufficient to fully analyse the effect of the impinging jet. Taking into account shear stress is therefore important to provide a more complete observation of the forces that bind a settled bed together. At a given critical value for τ_* , represents the instant at which motion of particles is initiated and erosion would occur.

MATERIALS AND METHODS

Materials

Soda lime glass spherical beads (SiO_2 , “Honite”, Guyson Internation Ltd, UK) of several size distributions were used as non-cohesive nuclear simulant waste for erosion experiments. Spherical glass was selected as the material of choice, as it is an ideal chemically inert particle to validate the experimental rig available in a large number of size ranges. Experiments were intended to provide useful baseline information when comparing other nuclear simulant materials in future studies. The used abbreviation for Honite is simply HX, where X represents the sieve size used by the manufacturer. Smaller values of X represent a larger sieve size.

Fig. 3 shows the size distribution of the glass particles, with vertical lines indicating their median D_{50} particle sizes. H8 representing the largest size distribution and H22 the smallest. D_{50} particle sizes ranging from 555 μm to 39 μm provides a comprehensive range to thoroughly investigate the effects size distribution has on erosion via impinging jet. These data were measured with a Malvern Mastersizer 2000.

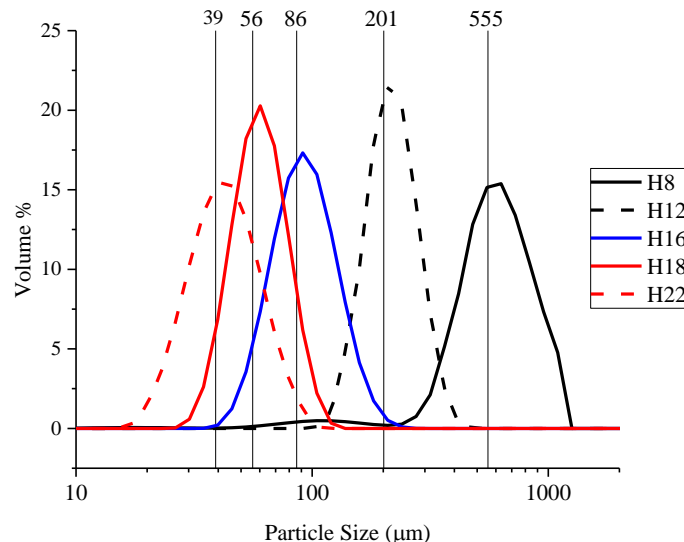


Fig. 3 Particle size distributions

Due to the reported size distribution of ZM as 0.1-100 μm [10], H22 shares its size distribution almost entirely with ZM and thus will provide the most interesting material of comparison as a non-cohesive simulant. Meaning it will be easy to identify at what point cohesive behaviour begins to directly affect erosion. Future testing will include a Barytes (BaSO_4) simulant, which is accepted as an appropriate inactive ZM simulant. Barytes has a very similar size distribution to ZM. This will allow for cohesive and non-cohesive comparisons to be made much more thoroughly [19].

Experimental

To define the strength of the sediment beds, the Yield stress of the Honite was measured using a Brookfield DV2T EXTRA viscometer. Sample preparation included creating a fully saturated beaker of Honite of each size distribution of the same volume fraction (~60%), which is representative of the porosity of the loose-packed bed within the erosion rig. Full saturation was achieved by adding the minimum volume of water to the Honite until the water barely covered the top layer of Honite. Two different vane spindles were used with the viscometer: V-74 (length: 11.76 mm, radius: 2.95 mm) and V-75 (length: 16.0 mm, radius: 4.02 mm). An average of 3 runs for each spindle were taken. The vane spindles consist of four vanes, which are submerged until fully covered in material, trapping glass between each vane forming a pseudo-cylinder of particles. The viscometer begins ramping up linearly to 0.5 RPM. The viscometer records the percentage of maximum torque required to initiate motion, the greatest value representing the yield stress of the particles [20]. The modified Shields parameter was calculated using the yield stress values (in place of normally quoted surface shear stress).

The erosion experiments took place in a 0.5 m^3 cubic tank, with 8 interchangeable jet nozzles, ranging from 2.5 mm to 9.5 mm, providing jet velocities from 5.1 ms^{-1} to 0.4 ms^{-1} , with respective Reynolds numbers 14234.9 – 3746.0. For each Honite size distribution, a bed of ~30 mm in height was added to the tank. The tank was filled with water to allow for complete submergence of the impinging jet. The Honite materials was thoroughly agitated and mixed, and allowed to settle completely, resulting in as close as possible uniformly settled bed. The jet height was initially set to 10d (where d again represents the jet diameter) above the surface of Honite, correlating with the approximate height of the jets in the HASTs [2] and as a compromise distance from 6d of the potential jet core [15] and area of effect on the bed. The impinging jet was fed by a peristaltic pump, run at its maximum flow rate (1.49 L/min). The jet was run for 5 minutes for each jet diameter, where the static erosion crater diameter (representing the crater size with the jet switched off) was measured. For each further experiment, the bed was then fully reset (re-suspended through vigorous agitation, and allowed to resettle), before testing repeated with a larger jet nozzle diameter. Experiments were also repeated for a height of 20d.

RESULTS AND DISCUSSION

For non-cohesive particles with the same density, physically larger particles should require more force to move as they simply have more mass per particle. However the smaller particle size distributions could fit more particles into the same volume as the larger, and could feasibly have the higher yield stress. Fig. 4 shows that the yield stress is in fact largest for the largest size distribution (H8) and trends downwards for the smallest (H22).

Assuming Honite is entirely non-cohesive, the trend suits the prediction, with decreasing yield stress as the size distribution decreases. However, the yield stress for H22 is noticeably higher than that for H18. Suggesting a greater number of particles in the same volume is a significant factor past a certain threshold or the H22 size distribution is small enough that interparticular forces are beginning to become significant, or a combination of the two. This behaviour has been observed to be unexpected previously. Matching experimental observations from Fig. 4 and Fig 5. show that factors such as coordination and more than individual particle inertia are responsible for yield stress in finer non-cohesive material [21, 22]. H16 fits

the expected trend but may be anomalous due to the large error bar present. The cause of this is at present still under investigation, however is included here for further discussion with erosion data. The modified

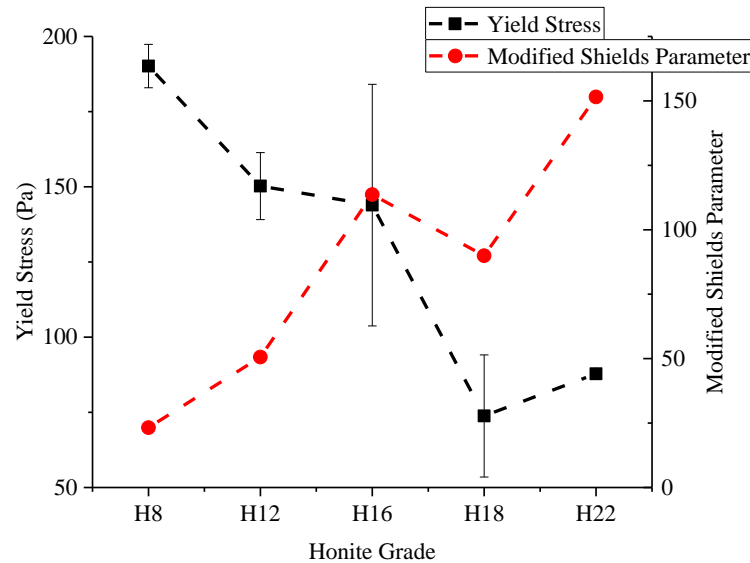


Fig. 4 Yield stress and Modified Shields Parameter of Honite

Shields parameter is simply the inverse of the yield stress trend, due to yield stress being divided by particle properties in Eq. 2.

As with the yield stress, the erosion experiments show some unexpected behaviour for non-cohesive particles. Fig. 5 show E_c vs. normalised erosion radius over jet height:

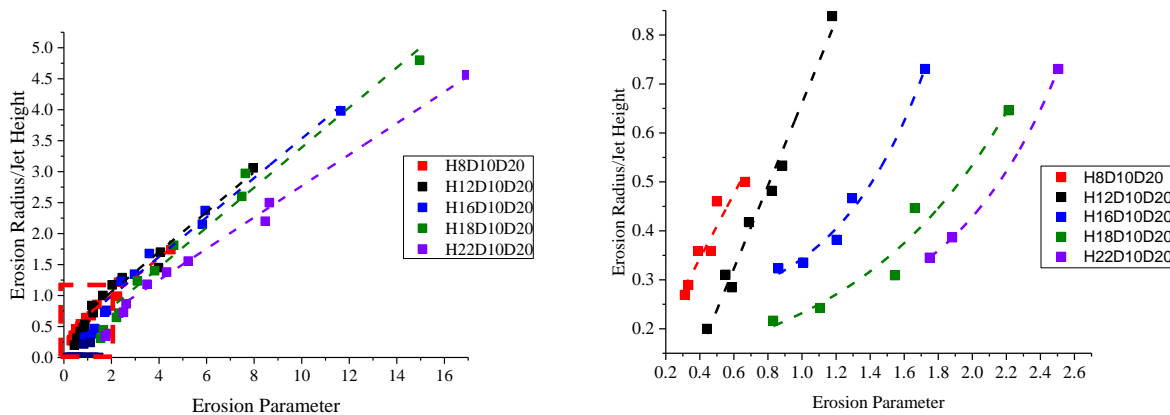


Fig. 5: E_c versus normalised erosion radius. (Left hand side, LHS) complete erosion profile. (Right hand side, RHS) Behaviour at low erosion parameters, $E_c < 3$, highlighted by dashed box.

As discussed $E_c > 2.0$ is considered to be the SDJR (i.e. more erosion due to penetration of the bed), and $E_c < 2.0$ the WDJR (i.e. less erosion due to less or no penetration of the bed) [14]. This two-regime pattern can be distinguished in Fig. 5 from LHS to RHS. Fig. 5 LHS shows $E_c > 2.0$ all data have linear gradients, which is expected for non-cohesive material. The yield stress data presented in Fig. 4 correlates with the greatest value of erosion radius for each data set, the higher the yield stress the less erosion (H8 greatest yield stress, lowest erosion radius. H18 lowest yield stress thus greatest erosion radius). Fig. 5 RHS should

WM2019 Conference, March 3 – 7, 2019, Phoenix, Arizona, USA

show a second linear region representative of the WDJR with steeper gradient than the SDJR. This can be seen for H8 and H12, however this is not the case for the remaining data, which is not expected for non-cohesive material.

At $E_c > 2.0$, H8 to H18 almost collapse onto a single line. H22 deviates significantly, giving further evidence that interparticular forces are significant. H8 and H12 display expected behaviour for non-cohesive particles [11, 16], maintaining a linear correlation in the WDJR. H16, H18 and H22 all display an exponential relationship in the WDJR. At such low E_c values, this could be explained by the jet not having the required energy to penetrate the bed and partially compressing the bed before shearing the surface, or that interparticular forces effect more than just the H22 as suspected. This observation is normally seen as a result of pH alteration introducing surface charge [23], suggesting that the glass particles might possess a partial surface charge at neutral pH and that it is becoming significant at the smaller size distributions.

CONCLUSIONS

H16 and H18 show some similar possible cohesive behaviour as H22 at lower E_c , showing that size distribution contributes significantly to erosion behaviour. The data presented begins to show where size distribution is no longer the only contributing factor, and interparticular forces possibly start to become a greater factor in non-cohesive material. This provides very useful comparison data for further investigation with cohesive materials considering they will certainly have significant cohesive forces arising beyond just Van der Waals forces. The cohesive materials will include barytes with similar size distributions to H22 as discussed, which makes the H22 in particular highly valued comparative data. This will provide a firm underpinning as to how the highly active liquor precipitates (ZM and CPM) might be behaving within the HASTs. Further to the barytes, titania (TiO_2) simulants is also to be considered for further cohesive comparisons. With a background of how non-cohesive material behaves under the influence of the impinging jet, trends and differences in behaviour of the cohesive material will be much more apparent.

Further experimentation is to be carried out utilising ultrasonic velocity profiling to more accurately measure erosion radius and depth with acoustic backscatter. In the cohesive systems the influence of the impinging jet will generate an opaque suspension, rendering visual analysis impossible.

REFERENCES

- [1] K. JAY, *Calder Hall The Story of Britain's First Atomic Power Station*, Jarrold and Sons Ltd, Norwich UK, 1956.
- [2] G. A. H. MCARTHUR, T. P. TINSLEY and D. MCKENDRICK, AICHE Annual Meeting, Conference Proceedings, Cincinnati, OH, USA, 2005.
- [3] H. PATERSON and M. IMGRAMS, Novel Glass Formulations for Post Operational Clean Out of Highly Active Storage Tanks, WM2017 Conference, March 5–9, 2017, Phoenix, Arizona, USA.
- [4] S. THOMSON, Progress in Defining the UK Highly Active Storage Tanks POCO Strategy, WM2016 Conference, March 6 – 10, 2016, Phoenix, Arizona, USA.
- [5] F. J. TURVEY and C. HONE, Storage of Liquid High-Level Waste at Sellafield: An Examination of Safety Documentation, 2000
- [6] N. PAUL, PhD Thesis, University of Leeds, 2014.
- [7] J. SHIELS, D. HARBOTTLE and T. N. HUNTER, *Materials* (Basel), 2018, **11**.
- [8] S. THOMSON, T. WARD, B. DUNNETT, R. ROBERTS and J. CHEESEWRIGHT, Recent Progress in the Understanding of UK Highly Active Liquor Chemistry and Properties, WM2017 Conference, March 5 – 9, 2017, Phoenix, Arizona, USA.
- [9] T. J. CRAFT, L. J. W. GRAHAM and B. E. LAUNDER, *International Journal of Heat and Mass Transfer*, 1993, **36**, 2685-2697.

WM2019 Conference, March 3 – 7, 2019, Phoenix, Arizona, USA

- [10] N. PAUL, S. BIGGS, M. EDMONDSON, T. N. HUNTER and R. B. HAMMOND, *Chemical Engineering Research and Design*, 2013, **91**, 742-751.
- [11] K. A. MAZUREK and T. HOSSAIN, *Canadian Journal of Civil Engineering*, 2007, **34**, 744-751.
- [12] A. ANSARI, S. U. KOTHYARI and K. RANGA RAJU, *J. Hydraul. Eng.*, 2003, **129(12)**, 1014-1019.
- [13] M. HADZIABDIC and K. HANJALIC, *Journal of Fluid Mechanics*, 2008, **596**, 221-260.
- [14] O. O. ADERIBIGBE and N. RAJARATNAM, *Journal of Hydraulic Research*, 1996, **34**, 19-33.
- [15] S. BELTAOS and N. RAJARATNAM, *Journal of Hydraulic Research*, 2010, **15**, 311-326.
- [16] T. N. HUNTER, J. PEAKALL, T. J. UNSWORTH, M. H. ACUN, G. KEEVIL, H. RICE and S. BIGGS, *Chemical Engineering Research and Design*, 2013, **91**, 722-734.
- [17] S. BADR, G. GAUTHIER and P. GONDRET, *Physics of Fluids*, 2014, **26**, 023302.
- [18] E. H. ZUBELDIA, G. FOURTAKAS, B. D. ROGERS and M. M. FARIAS, *Advances in Water Resources*, 2018, **117**, 98-114.
- [19] J. BUX, T. HUNTER, N. PAUL, J. DODDS, D. RHODES, J. PEAKALL and S. BIGGS, *In Situ Characterization of Mobilization, Dispersion and Re-Settling in Impinging Jet Ballast Tanks with an Acoustic Backscatter System*, WM2014 Conference, March 2 – 6, 2014, Phoenix, Arizona, USA.
- [20] N. Q. DZUY and D. V. BOGER, *Journal of Rheology*, 1985, **29**, 335-347.
- [21] P. C. KAPUR, P. J. SCALES, D. V. BOGER and T. W. HEALY, *AIChE Journal*, 1997, **43**, 1171-1179.
- [22] C. ANCEY and H. JORROT, *Journal of Rheology*, 2001, **45**.
- [23] Z. ZHOU, M. J. SOLOMON, P. J. SCALES and D. V. BOGER, *Journal of Rheology*, 1999, **43**, 651-671.

ACKNOWLEDGEMENTS

The authors would like to thank the Engineering and Physical Sciences Research Council (EPSRC) under grant number 1647979, The University of Leeds, The University of Manchester and Next Generation Nuclear – Centre for Doctoral Training are thanked for their funding and facilities for this research both past and current.